RESEARCH ARTICLE

Formulation, Optimization and Evaluation of Pentoxifylline-Loaded Microsponge Based Gel: A Synergistic *in vitro* and *in vivo* Approach for Accelerated Wound Healing in Albino Wistar Rats

Kirti Rajput[1], Dr. Sushant Kumar[2*], Dr. Amita Singh[3], Anurag Jaiswal[4], Dr. Praveen Kumar[5], Pritam Agrahari[6]

[1,2*,4,5,6]*Department of Pharmaceutics, Faculty of Pharmacy, Uttar Pradesh University of Medical Sciences, Saifai, Etawah, Uttar Pradesh, India.*

[3]*Veterinary officer & In-charge Animal House, Uttar Pradesh University of Medical Sciences, Saifai, Etawah, Uttar Pradesh, India.*

**Corresponding author-*

Dr. Sushant Kumar

**Email: k.sushant25@gmail.com*

Received- 15 Oct 2026 | Revised- 21 Oct, 2026 | Accepted- 29 oct 2026 | Available Online- 04 Nov 2026

ABSTRACT

Chronic and slow-healing wounds need topical therapy that keeps the drug at the wound site for a prolonged period. Pentoxifylline (PTX), a haemorheological agent with anti-inflammatory activity, has low oral bioavailability and a short half-life, which limit its systemic use for wound healing. This study aimed to develop PTX-loaded ethyl cellulose microsponges (PTX-MSPs) incorporated into a Carbopol gel (PTX-MSPG) for topical wound therapy. The microsponges were prepared by the quasi-emulsion solvent diffusion method and optimised using a two-factor, three-level central composite design, with the amount of ethyl cellulose and the volume of dichloromethane as independent variables and production yield, particle size and entrapment efficiency as responses. The optimised showed an entrapment efficiency of 88.6 ± 0.8%. FTIR, DSC, zeta potential and SEM analyses indicated that the drug was entrapped in spherical, porous microsponges in a non-crystalline state. The gel was translucent and washable, with a pH of 6.05 ± 0.04, a viscosity of 105 Pa·s, a spreadability of 6.41 ± 0.06 cm, a gel strength of 127 s and a syneresis of 0.63% w/w. In vitro release was biphasic, with 82.00% of the drug released from F7 over 24 h, and the data best fitted the Korsmeyer-Peppas model ($R^2 = 0.9666$, $n = 0.6332$), indicating anomalous (non-Fickian) transport. The gel remained stable for 3 months and was non-irritant to rat skin (primary irritation index 0.33, compared with 6.83 for formalin). In an excision wound model in Wistar rats, PTX-MSPG achieved 98.01% wound contraction on day 21, compared with 67.88% in untreated wounds, 69.95% with the blank microsponge gel and 91.15% with a conventional PTX gel, and histopathology showed re-epithelialisation with mature, organised collagen. These results suggest that the PTX-loaded microsponge gel is a safe, stable and sustained-release topical system that accelerates wound healing.

Keywords: Pentoxifylline, microsponges, ethyl cellulose, quasi-emulsion solvent diffusion, wound healing, excision wound model

How to cite this article: Kirti Rajput, Dr. Sushant Kumar, Dr. Amita Singh, Anurag Jaiswal, Dr. Praveen Kumar, Pritam Agrahari, "Formulation, Optimization and Evaluation of Pentoxifylline-Loaded Microsponge Based Gel: A Synergistic *in vitro* and *in vivo* Approach for Accelerated Wound Healing in Albino Wistar Rats" Int J Drug Deliv Technol. 2026;16(90s): 501-522; DOI: 10.25258/ijddt.16.90s.47

INTRODUCTION

A wound is a disruption of the normal structure and function of the skin. It may result from mechanical trauma such as abrasions and incisions, chemical agents, thermal injury such as burns, or biological insults [1]. Depending on the time and complexity of repair, wounds are classified as acute or chronic [2]. Acute wounds usually pass through the haemostatic, inflammatory, proliferative and remodelling phases in an orderly and timely manner. Chronic wounds, such as diabetic foot ulcers, venous leg ulcers and pressure sores, heal much more slowly because of persistent infection, underlying systemic disease or poor wound management [3]. Wounds place a substantial burden on patients and health care systems worldwide [4]. In a community-based survey in India, the prevalence of wounds was 15.03 per 1000 population, with 10.55 per 1000 for acute wounds and 4.48 per 1000 for chronic wounds [5], and a more recent community-based study reported a chronic wound prevalence of 1.89 per 1000 [6].

Topical therapy is attractive for wound care because the drug is delivered directly to the injured site, systemic exposure is reduced and patient compliance is improved. Conventional gels, creams and ointments, however, usually release the drug as an initial burst, need frequent application and may cause local irritation or absorption into the systemic circulation when the drug concentration at the application site is high [7,8]. A carrier that holds the drug and releases it gradually at the wound site is therefore desirable.

Pentoxifylline (PTX), chemically 3,7-dimethyl-1-(5-oxohexyl)-3,7-dihydro-1H-purine-2,6-dione, is a methylxanthine derivative used as a haemorheological agent in peripheral vascular disease [9]. It lowers blood viscosity, increases erythrocyte flexibility and improves tissue microcirculation, and it suppresses the production of tumour necrosis factor-α, a key pro-inflammatory mediator

[9,10]. These actions favour wound healing, and a Cochrane review found that PTX increased the healing of venous leg ulcers [11]. However, oral PTX has low and variable bioavailability because of extensive first-pass metabolism and a short plasma half-life, so frequent dosing is needed [9,12]. Delivering PTX directly to the wound in a sustained-release topical system could provide a local effect with lower systemic exposure.

Microsponges are porous, cross-linked polymeric microspheres, usually 5-300 µm in size, whose network of interconnected voids acts as a reservoir for the active ingredient [7,13,14]. The drug is released gradually by diffusion through the pores, which prolongs its action at the target site, lowers the dose needed and reduces side effects and irritation [7,8]. Microsponges are stable over a wide pH range (1-11) and at temperatures up to 130 °C, are compatible with many vehicles and, because their pores are smaller than bacteria, do not require sterilization or added preservatives [8,14]. Microsponge-based gels have been developed for mupirocin [15], clindamycin [16] and an immunosuppressant for psoriasis [17], and a mupirocin-loaded nanosponge gel has been evaluated for diabetic foot ulcers [18].

Microsponges can be prepared by the quasi-emulsion solvent diffusion (QESD) method, in which the drug and polymer dissolved in a volatile organic solvent are emulsified into an aqueous phase containing a stabiliser, and the solvent then diffuses out to leave porous, rigid particles [19-21]. Particle size, porosity and entrapment depend on formulation and process variables such as the polymer amount, solvent volume, stabilizer concentration and stirring conditions [19]. Ethyl cellulose (EC) is an inert, biocompatible, water-insoluble polymer that is widely used to form controlled-release matrices [22], which makes it a suitable structural polymer for microsponges. Because several variables interact, a statistical design such as the central composite design (CCD) allows optimization with a limited number of experiments [23].

We therefore aimed to develop PTX-loaded EC microsponges (PTX-MSPs) by the QESD method using polyvinyl alcohol as the stabilizer, to optimize the polymer amount and solvent volume with a CCD, and to incorporate the optimized microsponges into a Carbopol gel (PTX-MSPG). The microsponges were characterized by FTIR, DSC, zeta potential and SEM, and the gel was evaluated for its physical properties, in vitro drug release and release kinetics, stability and skin irritation. The wound healing potential of PTX-MSPG was then compared with a conventional PTX gel, the blank microsponge gel and no treatment in an excision wound model in Wistar rats, with measurement of wound contraction and histopathology.

MATERIALS AND METHODS

Materials

The materials required for the present work were procured from diverse sources. Pentoxifylline drug was procured as a gift sample from Bakul Pharm Fine Labs, Mumbai, Maharashtra. Ethyl cellulose, Carbopol 934 and Polyvinyl alcohol was purchased from Central Drug House, New Delhi. All the solvents and other chemicals used were of analytical grade.

Methods

Preparation of microsponges

The microsponges of PTX were synthesized by a quasi-emulsion solvent diffusion method by varying polymer and solvent concentrations. It involved the preparation of two phases inner phase and outer phase. The inner phase is made by dissolving the required amount of pentoxifylline and ethyl cellulose (0.1–0.3% w/v) in dichloromethane (DCM) (10–20 ml). A sufficient amount of magnesium stearate is added to the solution which act as a droplet stabilizer in the formulation of microsponges. The outer phase is prepared as aqueous solution of polyvinyl alcohol (PVA) (0.1%w/v). With continuous magnetic stirring of 600 rpm at room temperature, the inner phase is gradually introduced to the outer phase. Stirring causes the development of quasi-emulsion globules, which are discrete emulsion globules. The stirring was kept going for another 2 h till the insoluble stiff microsponges developed. Then, the solution was filtered, and the obtained microsponges were dried in an air-heated oven at 40 °C [21].

Table 1: Composition of Pentoxifylline loaded microsponges (PTX-MSPs)

Ingredients	F1	F2	F3	F4	F5	F6	F7	F8	F9	F10	F11	F12	F13
Pentoxifylline (mg)	100	100	100	100	100	100	100	100	100	100	100	100	100
Ethyl cellulose (ml)	400	400	400	400	600	400	600	200	400	200	117.15	682.84	400
Polyvinyl alcohol (% w/v)	0.5	0.5	0.5	0.5	0.5	0.5	0.5	0.5	0.5	0.5	0.5	0.5	0.5
Magnesium stearate (% w/v)	3	3	3	3	3	3	3	3	3	3	3	3	3
Dichloromethane (ml)	15	15	15	7.92	10	15	20	20	22.07	10	15	15	15
Distilled water (ml)	100	100	100	100	100	100	100	100	100	100	100	100	100

Optimization of pentoxifylline loaded microsponges

The microsponge is basically prepared using quasi ESD method and there are several formulation and processing variables like drug: polymer ratio, stirring time, stirring speed, internal phase volume, amount of emulsifying agent etc. which affects the process of microsponge formation. Ultimately these parameters effect on the critical quality attributes resembling Production yield, Mean particle size, Entrapment efficiency of final formulation. For the preliminary studies, first we have optimized the concentration of polymer and volume of dichloromethane, while the amount of drug and external phase volume was kept constant in each study trial. After finalizing the optimized value of those variables, their effect on the formulation was checked. The effect of different concentration of ethyl cellulose using 200, 400 and 600 mg and the effect of different volume of dichloromethane (10, 15 and 20 ml) on production yield, particle size and entrapment efficiency were also investigated.

A Central composite design was used to optimize PTX microsponges. Total of thirteen formulations of PTX MSPs were prepared by varying two independent factors. The polymer amount (X_1) and solvent (X_2) were considered as independent variables whereas % production yield (Y_1), particle size (Y_2) and percentage drug entrapment efficiency (Y_3) were considered as dependent responses. The effect of various independent variables upon dependent responses were modeled using following mathematical model equation generated by central composite design.

$$Y = b_o + b_1X_1 + b_2X_2 + b_{12}X_1X_2 + b_{11}X_1^2 + b_{22}X_2^2 \quad (1)$$

The experimental design was validated by preparing the three batches of optimized formulations. The responses of optimized formulations were evaluated. The predicted values were compared with experimental values and the % of bias was estimated [23].

Table 2: Selecting variables for optimization of microsponges

Independent Variables	Levels			Constraints
	Low (-1)	Medium (0)	High (+1)	
A: Concentration of Ethyl cellulose (mg)	200	400	600	In the range
B: Volume of Dichloromethane (ml)	10	15	20	In the range
Dependent Variables				
Y1: Production yield				Maximize
Y2: Particle size				Minimize
Y3: Encapsulation efficiency				Maximize

Evaluation of microsponges

Particle size

Particle size of microsponge was determine by optical microscopy using calibration ocular and stage micrometer under regular polarised light. A minute quantity of microsponge was spread on clean glass slide and average particle size was calculated by measuring 100 particles of each batch [20].

Production yield (PY)

The percentage yield was determined by determining the initial weight of the raw material used and the final weight of the microsponges and was estimated using the equation mentioned below [20].

$$\text{Production yield} = \frac{\text{Practical weight}}{\text{Theoretical weight}} \times 100 \quad (2)$$

Entrapment efficiency (EE)

PTX microsponges (10 mg) were dispersed in methanol, followed by shaking for 10 min using vortex mixer and the final volume made of 10 mL using methanol. The resulted solution was filtered, diluted and the concentration of PTX was determined spectrophotometrically using a spectrophotometer at 274 nm against a blank and tests were performed in triplicate [24].

Entrapment efficiency was calculated as per Eq. (3):

$$\%EE = \frac{\text{Weight of total drug} - \text{Weight of free drug}}{\text{Weight of total drug}} \times 100 \quad (3)$$

Zeta Potential

The zeta potential was determined using Zetasizer Nanoseries ZS (Malvern Instruments Ltd., UK). The measurements were monitored at room temperature after each formulation sample was diluted with ultrapure water (1:80, v/v) [24].

Fourier transform infrared (FTIR) analysis

FTIR spectra of the PTX, EC, physical mixture and drug loaded PTX were recorded in the scanning range of 600–4000 cm^{-1} at a resolution of 2 cm^{-1} with scan speed of 64 scan/s by using FTIR-8400S (JASCO, FTIR-4X (Type A). A small amount of each sample was softly ground with potassium bromide in a glass mortar to form a pellet. This pellet was placed into sample holder for analysis. The spectrum was recorded by using IR Solution software [16].

Differential scanning calorimetric (DSC) analysis

Thermal characteristics of PTX, EC, physical mixture and drug loaded MSPs were evaluated using DSC-60 (Shimadzu, Japan). Each sample (average weight taken 3 mg) was accurately weighed into aluminum pan and sealed hermitically by using a compressor and all the samples were subjected to thermal analysis. The thermograms were recorded at a heating rate of 10 °C/min from 10 °C to 300 °C under nitrogen atmosphere (flow rate 20 mL/min) [16].

Scanning Electron Microscopy (SEM) analysis

Prepared microsponges were subjected to scanning electron microscopy (SEM) analysis for assessing their morphology and surface topography. SEM (JSM-IT200, Jeol, Japan) analysis of MS particles revealed size, shape, and morphology. At first, particles were attached to a metal stub using conductive tape to create a conductive path and then shielded with a thin layer of platinum under lower pressure [19].

Preparation of the gel base and microsponge loaded gel

Forming polymer (Carbopol 934) was soaked in water for overnight and then dispersed by agitation at approximately 600 rpm with the aid of magnetic stirrer to get a smooth dispersion. The dispersion was allowed to stand for 15 min to expel entrained air. To it the aqueous solution of triethanolamine (2% v/v) was added with slow agitation for adjusting pH to 6.5–7.5. At this stage permeation enhancers and microsponges containing drug equivalent to marketed formulation were incorporated into the gel base. Prepared gels were packed in wide mouth glass jar covered with screw capped plastic lid after covering the mouth with aluminum foil and were kept in dark and cool place until use. 40 mg drug equivalent MSPs was taken and mixed gently with the 4 g gel base to obtain 4 g microsponge based gel [21].

Evaluation of PTX loaded microsponge based gel

Physical Characterization

After being packed into the container, the formulated gel's physical characteristics, color, and homogeneity were visually assessed.

pH measurement

The pH of the formulated gel was gauged using a pH metre (PH-01, Labioco, Athens, Greece) that had been calibrated with a pH 7 buffer prior to use. The electrode tip was immersed in the gel, and the reading was taken after 2 min. This pH measurement procedure was performed in triplicate, and the average value was computed [25].

Homogeneity and Grittiness

A tiny amount of gel was squeezed between the thumb and index finger to observe its consistency, whether it was uniform or not. In addition, the uniformity may be identified by applying a little amount of the gel over the skin of the dorsal side of the hand. The coarseness of the produced gel is also examined in a similar manner [25].

Viscosity measurement

Viscosity, which signifies a resistance of fluid to flow, was assessed using a Brookfield viscometer (AMETEK Brookfield, DV-II + Pro, India) equipped with spindle No. 7, operating at 12 rotations per minute (rpm) at room temperature (RT) [26].

Spreadability analysis

The spreadability was determined by method of horizontal plate glass. A similar weight (2 g) was attached to the upper glass plate, and between two horizontal glass plates about 1 g of the optimized PTX-MSP gel was mounted. It had been held upright. It was noticed the duration it took for the top glass plate to separate from the bottom glass plate. The formula below was used to determine the spreadability.

$$S = \frac{MxL}{T} \quad (4)$$

where, S = spreadability; L = length of glass slide (cm), M = weight of the upper slide (g), and T = time taken (sec) [27].

Drug Content

The prepared PTX-MSPG (1 gm) was dissolved into methanol and sonicated using a probe sonicator (Helix Bioscience, India). The sample was filtered using a membrane filter (0.22 µm), and the content was analyzed using a UV spectrophotometer after an appropriate dilution [28].

Determination of gel strength

A 30 mm stainless-steel ball was inserted into the center of 40 g of the gel, which was then permitted to pierce through the gel, into a 50 mL beaker. For every formulation, the duration required for the ball to pierce the gel five centimeters down was recorded. The measurement was repeated three times for each formulation [29].

Syneresis study

A fixed amount (10 g) of optimized D-MSPG formulation was subjected to the environmental condition of room temperature (~25°C/60 ± 5% RH) for one month. The percentage of water exudate from the gel was calculated [15].

***In vitro* drug release assay**

In vitro drug release investigations were conducted using Franz diffusion cells with a receptor chamber capacity of 13 mL and an effective diffusion area of 3.14 cm2. A cellulose dialysis membrane from Himedia, Mumbai, India, was soaked in the receptor medium (phosphate buffer, pH 5.8) for a period of 24 h prior to the commencement of the experiment. The donor side of the arrangement held a predetermined quantity of gel containing PTX-MSPs. During the experiment, the receptor solution was consistently agitated at 50 rpm and maintained at a steady temperature of 32 ± 0.5 °C through a circulating jacket. At specific intervals, 1 mL samples were withdrawn from the receiving compartment, and an equal volume of fresh buffer was introduced to ensure sink conditions. The extracted samples were subjected to analysis using a UV-Spectrophotometer to quantify the quantity of released PTX. The drug release data underwent linear regression analysis to determine the release kinetics, encompassing zero-order and first-order release kinetics, as well as the diffusion-controlled [18].

Release kinetics modelling

The drug release kinetics was examined using different kinetic models, namely the zero order, first order, Higuchi, and Korsmeyer-Peppas models. The *in vitro* drug release data were fitted to these models to find out the release pattern. The zero-order plot was drawn as the cumulative amount of drug released vs. time, the first order plot as the log cumulative percentage of drug remaining vs. time, and the Higuchi model as the cumulative percentage of drug released vs. the square root of time. The best-fitting model was identified by the correlation coefficient value closest to 1. The data are presented for the most suitable model.

Zero order: The Graph is drawn for cumulative amount of drug released vs. time

$$C = K_0 t \quad (5)$$

where K_0 is the zero order rate constant, expressed in concentration/time, and t is the time in hours. When concentration is plotted against time, a straight line is obtained, with K_0 as the slope and the intercept at the origin of the axes.

First order: The Graph is drawn for the log cumulative percentage of drug remaining vs. time

$$\text{Log } C = \text{Log } C_0 - kt/2.303 \quad (6)$$

where t is the time, C_0 is the initial concentration of the drug, and k is the first order rate constant.

Higuchi's model: The Graph is drawn for cumulative percentage of drug released vs. square root of time.

$$Q = Kt^{1/2} \quad (7)$$

where t is the time in hours and K is the constant that represents the design variables of the system. Consequently, the drug release rate is governed by the reciprocal of the square root of time.

Korsmeyer-Peppas: The widely used Korsmeyer-Peppas equation, which is often applied to describe drug release behavior from polymeric systems, was also fitted to the dissolution data (as log cumulative percentage of drug released vs. log time), and the exponent n was obtained from the slope of the straight line.

$$Mt/M\infty = Kt_n \quad (8)$$

where n is the diffusional exponent that explains the mechanism of drug release, K is a kinetic release rate constant specific to the drug/polymer system, Mt is the amount of drug released at time t, t is the release time, and Mt /Mꝏ is the fractional solute release.

The release mechanism is Fickian diffusion when the exponent n = 0.45, and non-Fickian or anomalous diffusion when n < 0.89. A typical zero-order release, or Case-II transport, is indicated by an exponent value of 0.89 [17].

Stability studies

The main objective of the stability testing is to provide evidence on how the quality of the drug product varies with time under the influence of temperature and humidity. The optimized PTX loaded microsponge based gel was stored in a sealed glass vial and subjected to the physical stability testing in triplicate as per International Conference on Harmonization (ICH) Q1A (R2) guidelines [30]. The vials were stored at 4 ± 2 °C with ambient humidity and room temperature 25 ± 2 °C. The stored samples were analyzed over 3 months at an interval of one month. PTX loaded microsponge based gel was estimated for physical appearance, pH, spreadability and drug content [31,32].

Skin Irritation investigation

The Institute Animal Ethical Board criteria were adhered to throughout the investigations. Wistar rats were shaved the day before the experiment to remove any hair from their dorsal regions. Group I was the control, Group II was given a 0.8% (v/v) water solution of formalin as the standard irritant, Group III received the blank microponge based gel and Group IV received PTX loaded microsponge based gel. For three days, standard topical formulation, formalin solution, blank microsponge based gel, PTX loaded microsponge based gel, were applied topically to the skin of rats. The affected area was examined visually throughout the time. This procedure is blinded for observers. After 72 hours, the sites of application were examined for edema and erythema and graded on a scale from zero to 4 based on visual assessment by the same blind investigator. Photographs were taken to document erythema observed at some application sites on rats. The Primary Irritancy Index (PII) for each group was determined using a specific calculation formula [33-35].

$$PII = \text{Mean score of erythema} + \text{Mean score of edema} \quad (9)$$

***In vivo* wound healing studies**

Wistar albino rats (either sex) in good health, weighing 200 and 275 g, were selected. The Institutional Animal Ethics Committee (Approval number IAEC/09/AH/2025-26) granted approval to the study protocol in accordance with Indian Committee for the Purpose of Control and Supervision of Experiments with Animals (CPCSEA) specifications. Throughout the study, animals were kept in a standard laboratory environment at a temperature of 25 ± 2 °C with a relative humidity of 44–56% and fed a standard diet and water.

Excision wound model

Every rat participating in the study was administered an intraperitoneal injection of ketamine hydrochloride at a dos age of 80 mg/kg to induce anaesthesia on the day designated for wound creation. The dorsal furs of animals were removed using deplicating cream [Veet hair removal cream, Reckitt benckiser (India) Ltd]. The wound development procedure involved creating a circular pattern on the dorsal side of the rat. Using a scalpel blade, a wound was created by separating a complete skin layer with a standardised dimension of 2 mm^2. The rats were then randomly distributed into various experimental groups for further study. The purpose of this experimental setup was likely to be to investigate wound healing or other related phenomena in response to different treatments or interventions.

Animal groups and treatment protocols

Rats were split into 4 groups (n = 6), with 6 rats in each group, and exposed to the subsequent treatment:

Group I: Wounds created but not treated (negative control group)

Group II: Wound treated with conventional PTX gel (positive control group)

Group III: Wound treated with microsponges based gel without drug.

Group IV: Wound treatment by optimized drug loaded microsponges based gel.

Treatments were started immediately after creating the wound on day 0 by daily application of above mentioned topical formulations on the wounded area. Day 0 is considered as a wounding day, when the wound was created first. One gram of each formulated gels and marketed formulation mentioned above was applied once daily from day O until complete healing to the respective groups.

Measurements of % wound contraction

The wounded area was monitored and measured using scale and the percentage contraction after every 4th day was calculated. The initial size of the wound was considered 100% using the following equation:

$$\%\text{Wound contraction} = \frac{\text{Initial wound area - Specific day wound area}}{\text{Initial wound area}} \times 100 \quad (10)$$

Histopathological evaluation of wounds

On the last day of the wound healing experiment, the animals were anesthetized using Ketamine HCl (50 mg/kg, i.p.), euthanized, and specimens of wound tissue with the adjacent healthy tissue were collected. The collected samples were fixed in 10% formalin and were subjected to routine histopathological tissue examination. The wound tissue specimen was sectioned with a microtome and then stained with hematoxylin-eosin. The prepared tissue slide was examined under a light microscope [36].

Statistical Analysis

All experiments were performed in triplicate. The data are represented as a mean ± standard deviation. Statistical analysis of the data was performed by two-way analysis of variance (ANOVA), followed by Tukey's post hoc test for multiple comparison using GraphPad Prism 8.0 software; a value of $p < 0.05$ were regarded to be statistically significant.

RESULTS AND DISCUSSION

In this study, we have developed and optimized PTX loaded microsponges (MSPs), integrating these MSPs into the topical gel that offers several benefits. The innovative approach offers sustained release, reduced side effects, improved patient compliance and enhanced bioavailability, collectively contributing to more effective and tolerable treatment regimens for wound management.

Optimization studies of microsponges using Central composite Design (CCD)

A 2 factor, 3-level CCD was employed to optimize the formulation of PTX-MSPs. The factors under consideration included the concentration of EC and volume of DCM which were investigated to uncover their effects on the afore mentioned parameters. Table 2 present the coded levels of concentration of EC and volume of DCM that were utilized in the experimental design. The visual representation of the data is facilitated through the utilisation of two- and three-dimensional surface plots. These plots elucidate the relationships between variables and response out comes, these insightful visualisations are presented in Figures 1 and 2.

Table 3: Formulation optimization trial details and their effect of Ethyl cellulose and dichloromethane on production yield, mean particle size and EE

Run	Space Type	Factor A: Concentration of Ethyl cellulose	Factor B: Volume of Dichloromethane	Response 1: Production yield (%)	Response 2: Particle size (µm)	Response 3: Entrapment efficiency (%)
1	Centre	400	15	74± 0.7	251	77.1± 0.9
2	Centre	400	15	63± 0.85	258	76.8± 0.9
3	Centre	400	15	77± 0.75	158	85.4± 0.9
4	Axial	400	7.92893	61± 0.85	431	68.5± 0.7
5	Factorial	600	10	63± 0.72	193	80.02± 0.82
6	Centre	400	15	65± 0.81	163	77.5± 0.7
7	Factorial	600	20	79± 0.81	148	88.6± 0.8
8	Factorial	200	20	72± 0.75	167	68.9± 0.8
9	Axial	400	22.0711	75± 0.85	155	83.1± 0.9
10	Factorial	200	10	60± 0.72	211	62.3± 0.7
11	Axial	117.157	15	75± 0.72	184	59.8± 0.8
12	Axial	682.843	15	68± 0.81	364	77.35± 0.85
13	Centre	400	15	71± 0.81	208	78.16± 0.86

Effect on Production yield

The PY of PTX - MSPs was found to range from 60± 0.72 % 79± 0.81% for various factors and level combinations. For production yield, the mathematical is equation was established as:

$$Y_1 = 70 + 0.0126A + 5.97B + 1.0AB + 0.4375A^2 - 1.31B^2 \quad (11)$$

DCM volume (B) was the dominant factor (+5.97): a larger volume lowers the viscosity of the internal phase, keeps drug and polymer well dispersed, and favours uniform droplet formation and better microsponge recovery. The negative B^2 term (−1.31) shows the gain levelled off at higher volumes, probably because excess solvent diluted the system and delayed droplet solidification. Ethyl cellulose concentration (A) had a negligible linear effect (+0.0126), with only small contributions from A^2 (+0.4375) and the AB interaction (+1.0). The response surface and contour plots showed a steep rise along the B axis and a nearly flat profile along A. The stationary point was a saddle point outside the design space, with the highest predicted yield (≈ 76.1%) at high DCM volume

combined with the higher ethyl cellulose level. Overall, production yield was governed mainly by DCM volume, while ethyl cellulose played a minor role.

Effect on Particle size

The PS of PTX - MSPs was found to range from 148 µm to 431 µm for various factors and level combinations. For a particle size, the linear model equation was represented as:

$$Y_2 = 207.6 + 27.19A - 59.9B - 0.2500AB + 7.26A^2 + 16.76B^2 \quad (12)$$

DCM volume (B) was the dominant factor (−59.9): a larger volume lowers the viscosity of the internal phase, so droplets break up more easily under agitation and solidify into smaller microsponges. Ethyl cellulose concentration (A) had a positive effect (+27.19), since higher polymer content raises viscosity, resists droplet break-up and gives larger particles. The positive quadratic terms (A^2, +7.26; B^2, +16.76) indicate curvature, with the reduction in size flattening at higher DCM volumes, while the negligible AB term (−0.25) shows the two factors acted almost independently. The response surface and contour plots showed the largest particles (≈ 319 µm) at high ethyl cellulose with low DCM volume and the smallest (≈ 145 µm) at low ethyl cellulose with high DCM volume, and because the stationary point (A ≈ −1.84, B ≈ +1.77) lay outside the design space, the minimum size was reached at the boundary. Overall, particle size was governed mainly by DCM volume, followed by ethyl cellulose concentration.

Effect on Entrapment efficiency

EE, an important factor in the successful encapsulation of active substances within a delivery system, is influenced by various independent variables. The impact of independent variables on EE is investigated in this study. The EE of PTX - MSPs was found to range from 59.8± 0.8% to 88.6 ± 0.8% for various factors and level combinations. Equation 14 illustrates the impact of independent factors on entrapment efficiency.

$$Y_3 = 78.992 + 7.77993A + 4.47844B + 0.495AB - 4.51662A^2 - 0.904125B^2 \quad (13)$$

Both factors had a positive linear effect on entrapment efficiency, with ethyl cellulose concentration (A, +7.78) stronger than DCM volume (B, +4.48). Higher polymer content gives a denser, more viscous internal phase that reduces drug diffusion into the external aqueous phase, while a larger DCM volume keeps drug and polymer well dispersed and favours uniform polymer deposition. The negative quadratic terms (A^2, −4.52; B^2, −0.90) indicate curvature, with the gain at higher polymer levels diminishing, probably because excess viscosity hinders uniform droplet formation, and the small AB term (+0.495) shows the factors acted almost independently. The response surface was dome-shaped, with the lowest entrapment (≈ 61.8%) at low A and low B and the highest (≈ 86.3%) at high A and high B; the stationary point (A ≈ +1.01, B ≈ +2.75) was a maximum but lay outside the region in B, so the best result within the studied range (≈ 86.4%) was at the upper DCM level with high ethyl cellulose. Overall, entrapment efficiency was governed mainly by ethyl cellulose concentration, with a smaller positive contribution from DCM volume.

As a result, the optimised microsponges batch (F7) was selected for further characterisation studies and incorporated into a Carbopol gel base. The findings from the central composite design and regression equations provide valuable insights for optimizing microsponge formulations with enhanced properties for potential pharmaceutical applications. The predicted theoretical values were very close to the responses produced by the experiments, indicating that the experimental design employed in the current study was robust (Table 4).

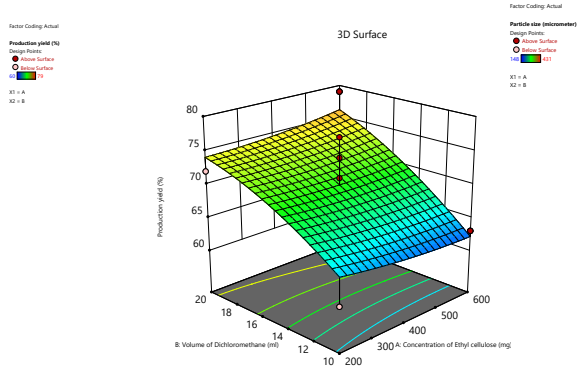

A

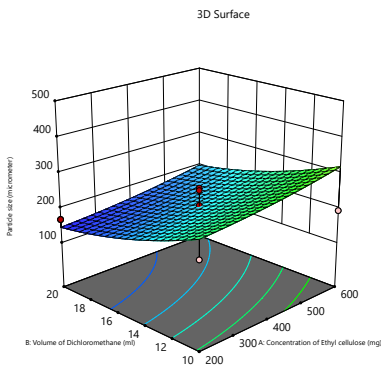

B

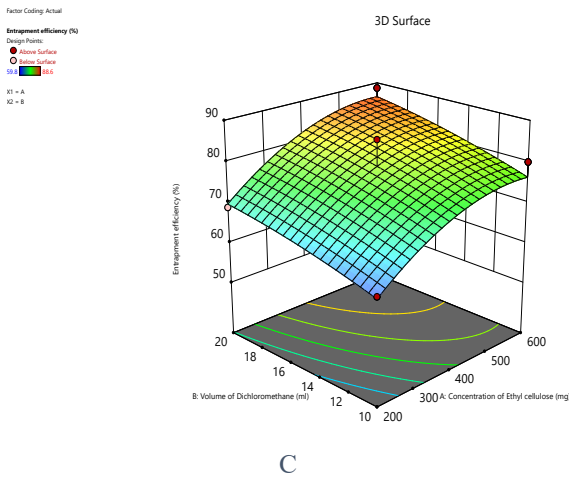

C

Figure 1: 3D contour plots of (A) Production yield (B) Particle size (C) Entrapment efficiency

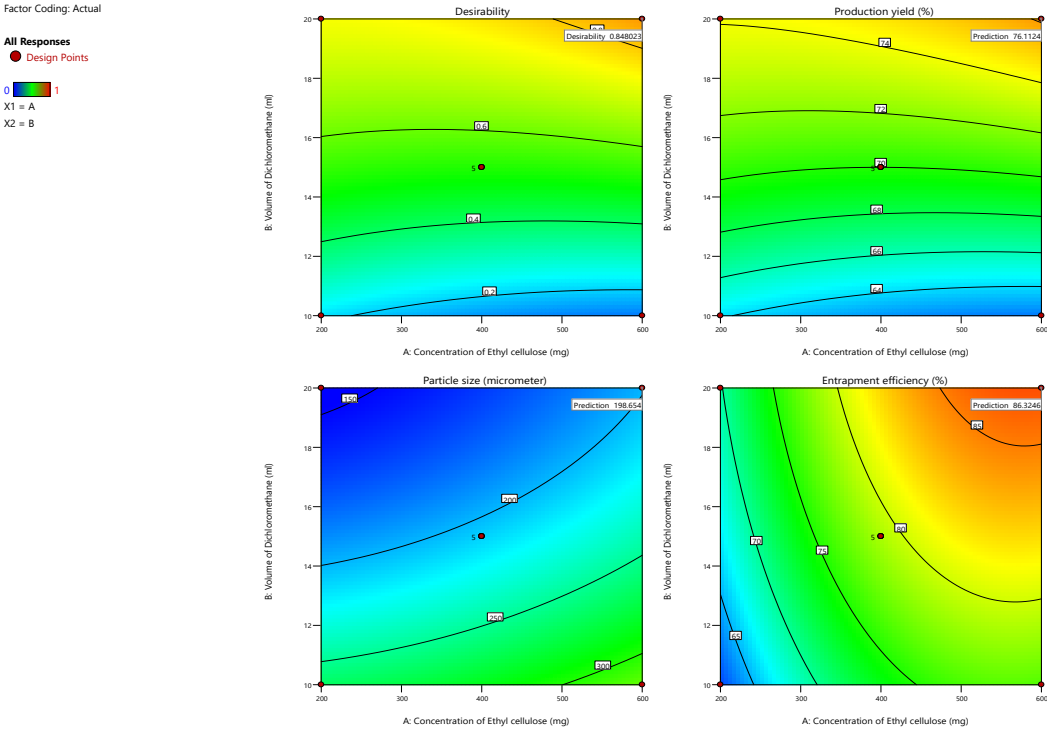

Figure 2: 2D contour plots of Desirability, Production yield, Particle size and Entrapment efficiency

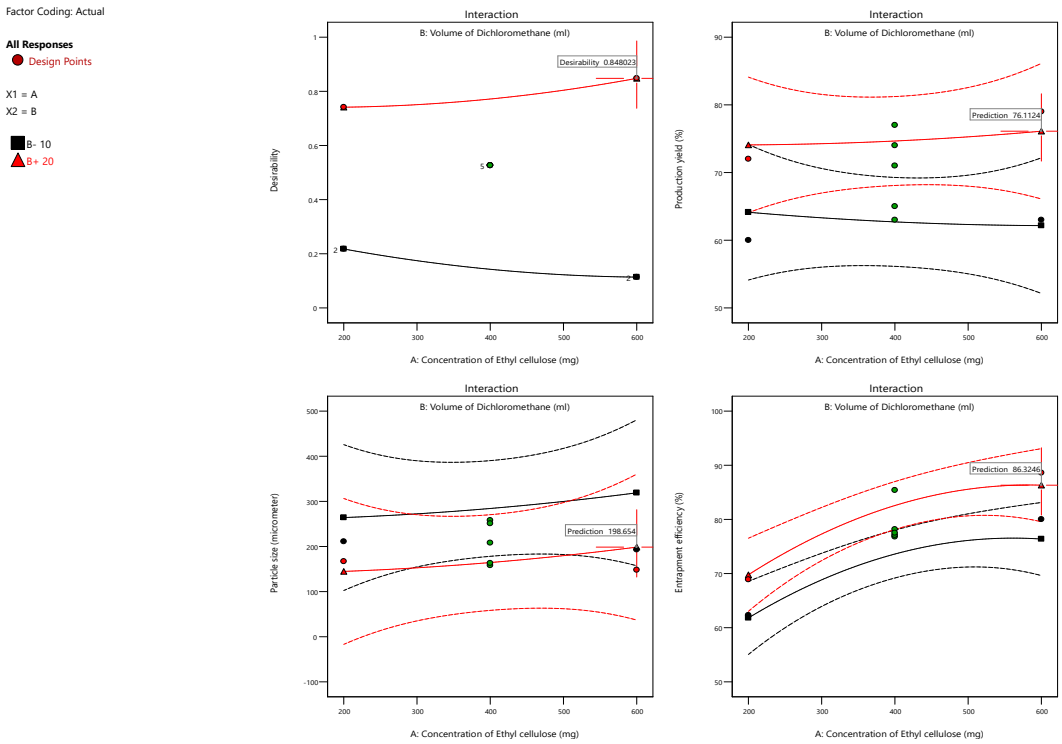

Figure 3: Interaction plots for Desirability, Production yield, Particle size and Entrapment efficiency

Table 4: Comparison between predicted and experimental values in the formulation prepared under predicted optimum conditions

Response	Predicted values	Experimental values	% Bias
Production yield (%)	154.7	148	4.53
Particle size (µm)	75.4	79	-4.56
Entrapment efficiency (%)	86.32	88.6	- 2.57

Characterization of Optimized PTX-MSPs Formulation

FTIR analysis

Figure 4,5,6 &7 shows the FTIR spectra of pentoxifylline, ethyl cellulose, the physical mixture, and optimized pentoxifylline loaded microsponges formulation (F7). The spectra of pure pentoxifylline drug show the characteristics peak at 1655 cm^{-1} for C=O stretching and 1546 cm^{-1} corresponds to C=N bending. The FTIR spectra of the physical mixture confirmed all characteristic peaks of pentoxifylline with no additional peaks. The characteristic peaks of pentoxifylline in the FTIR spectrum of MSPs disappeared. This suggests that the drug was completely encapsulated within MSPs. Overall, the FTIR spectra confirmed the entrapment of drug in the EC within the MSPs.

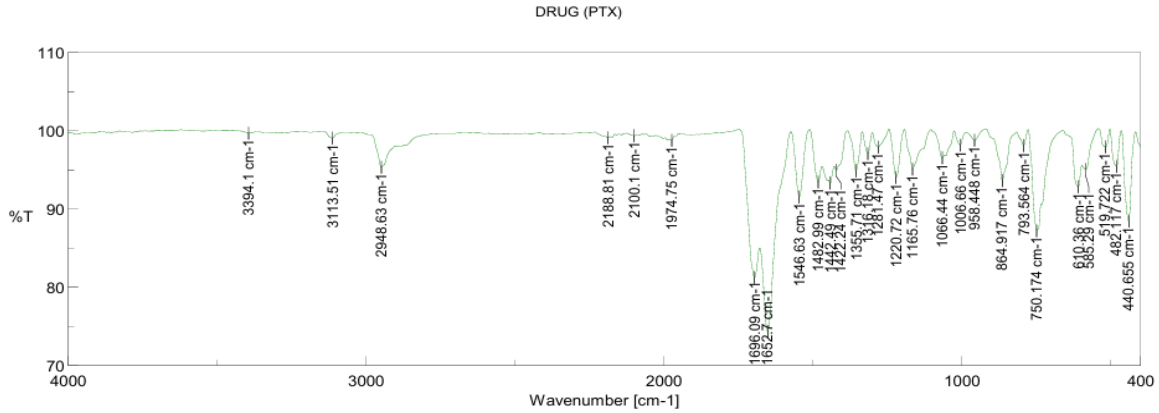

Figure 4: IR spectra of drug

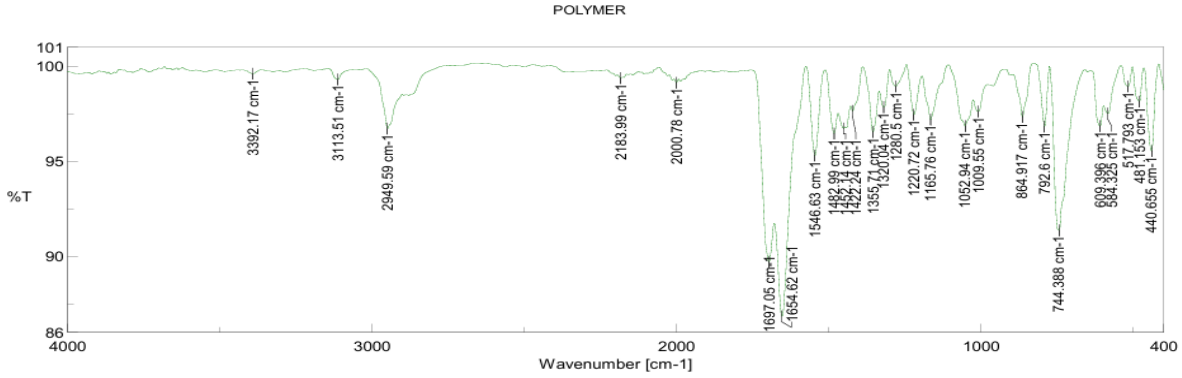

Figure 5: IR spectra of polymer

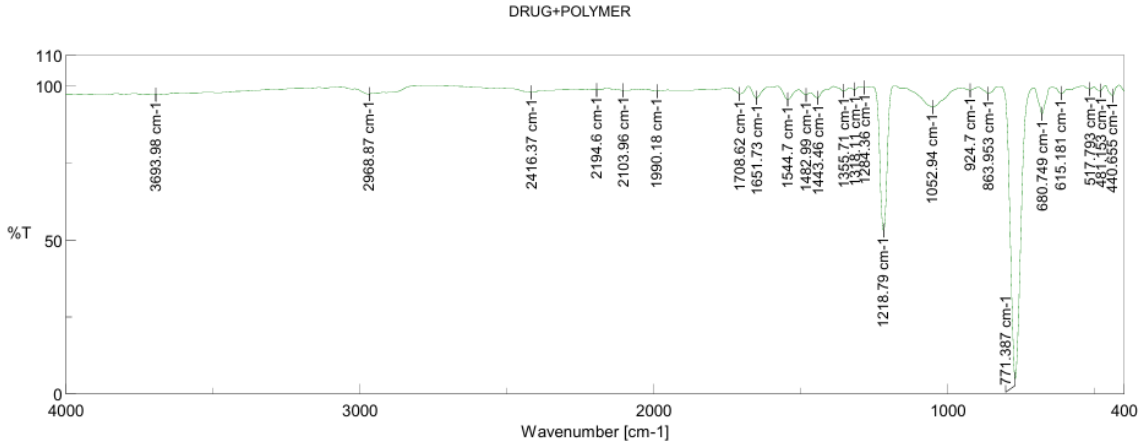

Figure 6: IR spectra of physical mixture of drug and polymer

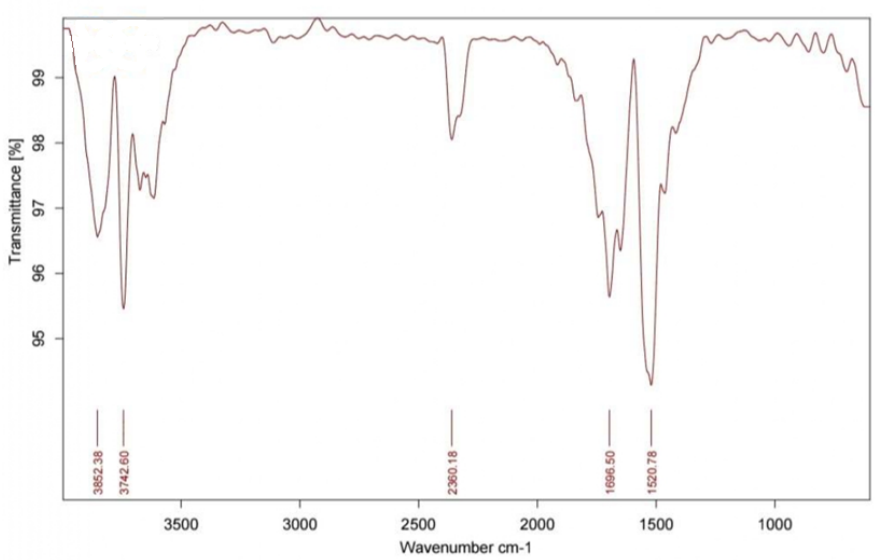

Figure 7: IR spectra of optimized PTX-MSPs

Zeta Potential Determination

The ZP value of the optimized PTX-MSPs (F7) was found to be - 3.23 mV, as shown in Fig.8. This slightly negative ZP value indicates minimal electrostatic repulsion among the dispersed microsponges. In polymeric microsponge systems, a low magnitude of zeta potential suggests that physical stabilization during storage is primarily governed by steric hindrance imparted by the polymeric matrix and surfactant coating rather than electrostatic charge stabilization. Incorporating these microsponges into a structured gel network will effectively prevent phase separation or particle sedimentation caused by weak electrostatic repulsion.

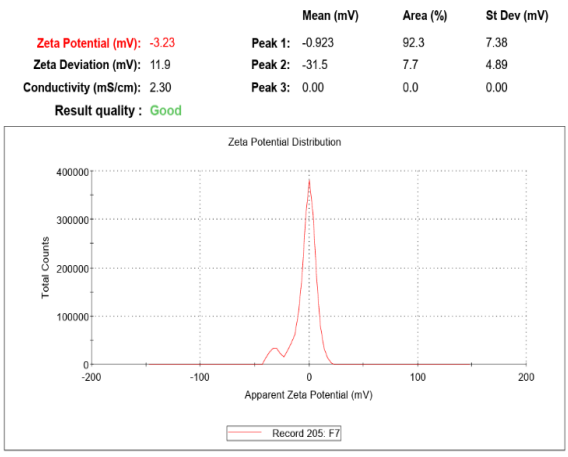

Figure 8: Zeta potential of optimized MSPs

Differential Scanning Calorimetry (DSC) analysis

The DSC thermogram of the PTX-loaded microsponges displayed a continuous baseline decline followed by a single endothermic transition at 81.0ºC (attributed to moisture loss and polymer matrix softening) as shown in Fig 9. Crucially, the sharp, high-enthalpy melting endotherm characteristic of crystalline pure PTX (220 -221 ºC) was completely absent, confirming that the drug was molecularly dispersed and converted into an amorphous/disordered state within the ethyl cellulose matrix.

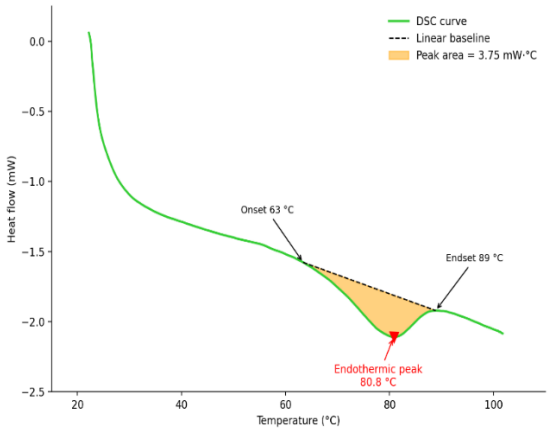

Figure 9: DSC thermogram of optimized PTX-MSPs formulation

Scanning Electron Microscopy (SEM) analysis

SEM photomicrographs in Fig.10 revealed that the microsponges were predominantly spherical, free-flowing, and highly porous, featuring an internal cavity enclosed by a rigid drug-polymer shell formed by solvent diffusion.

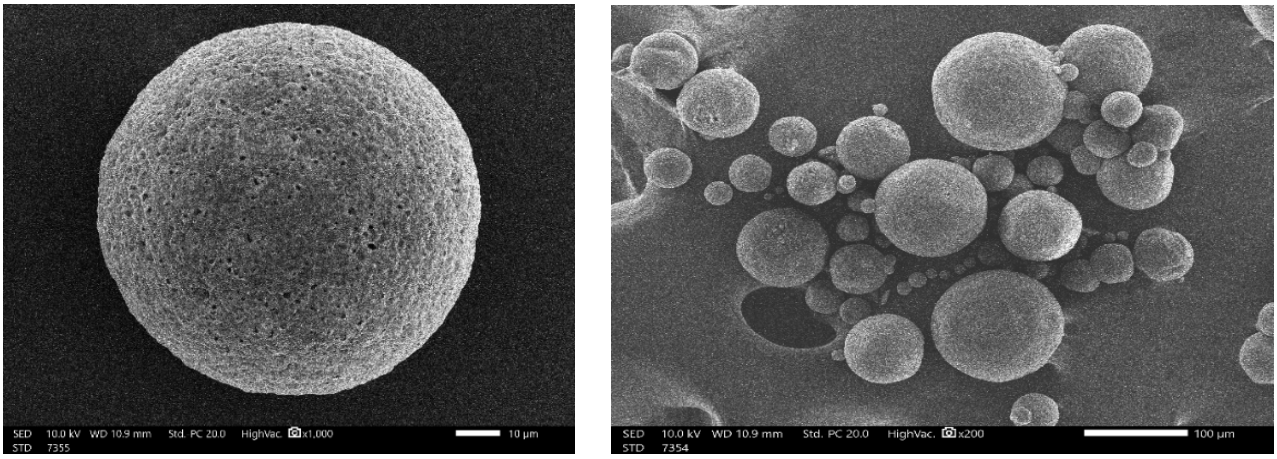

Figure 10: Illustration of SEM analysis of optimized PTX-MSPs formulation

Characterization of PTX-MSPG formulation

Physical Appearance

Prepared gel formulations were physically characterized for colour, clarity, odour and washability by visual inspection are given below in Table 5.

Table 5: Physical characteristics of gel

S.No.	Organoleptic Characteristics	Results
1.	Colour	Colourless
2.	Clarity	Translucent
3.	Odour	Odourless
4.	Washability	Washable
5.	Consistency	Good

pH determination

The pH of a topical formulation is one important parameter that needs to be fixed properly to avoid any kind of incidences like skin irritation, redness, or other adverse events. pH of the F7 batch was measured by using a digital pH meter, and the values were taken in triplicate for accurate measurement. The pH of the optimized gel formulation was found to be 6.05 ± 0.04.

Homogeneity and Grittiness

Upon visual inspection, the gel showed a smooth and uniform appearance throughout with no sign of phase separation, confirming that it is completely homogenous.Furthermore, when rubbed between fingers, the gel formulation was entirely free from coarse or particulate matter, indicating the absence of grittiness and ensuring a comfortable texture for topical application.

Viscosity determination

The viscosity of optimized PTX-MSPG formulation was found to be 22450± 310 cPs. It indicates sharp pseudoplastic (shear- thinning) topical gel structure. This consistency provides excellent retention at the application site and prevents the microsponges from settling during storage.

Spreadability study

The spreadability of a topical gel formulation is an important parameter to understand how easily the gel will spread on the application surface. The spreadability of the optimized PTX-MSPG formulation was 5.65 ± 1.03 g cm/s. This indicates a flexible gel matrix that can spread easily on the application surface

Determination of gel strength

Products like gels, capsules, and contact lenses are developed based on their strength, flexibility, and rupture force. Gel strength is a measure of a colloidal dispersion's capacity to form and sustain a gel form. Strong gels will withstand far greater pressure than weak gels before being flushed from the site of administration, and it will affect the spreadability and drug's release. The gel strength of the optimized PTX-MSPG was found to be 127 seconds.

Syneresis study

network. This process continues until the repulsive forces in the gel structure are arrested. The extent of syneresis is dependent on the concentration of the gelling agent. As the amount of gelling agent decreases, the chance of syneresis will increase. Further, the phenomenon is related to the elastic stress relaxation which developed during the gel setting. Since the stress is relieved, the availability of interstitial space will be reduced which further accelerates the process of fluid oozing from the gel matrix on storage. For optimized PTX-MSPG formulation, syneresis was observed to be 0.63% w/w. According to a literature report, a syneresis near 7% w/w is considered a high syneresis. Compared to the literature report, PTX-MSPG formulation showed minimum syneresis. Syneresis of gel is a phenomenon where the gel network shrinks itself oozing out the arrested fluid from the gel.

***In vitro* drug release assay**

The *in vitro* drug release profiles of the formulations F3, F7 and F9 over 24 h are shown in Fig. 11. All three formulations showed a biphasic release pattern, with an initial rapid release followed by a slower, sustained release. In the first 0.5 h, F3 released 12.33%, whereas F7 and F9 released 7.85% and 8.41%, respectively. This initial burst is most likely due to drug adsorbed on the surface of the microsponges or present in the gel base, which dissolves immediately on contact with the release medium. After this phase, release was controlled mainly by diffusion of the drug through the porous microsponge network and the surrounding gel matrix. At 10 h, the cumulative release was 70.14% (F3), 69.36% (F7) and 73.62% (F9). The time for 50% release was approximately 5.4 h for F3, 5.6 h for F9 and 5.9 h for F7. At 24 h, the cumulative release was 87.25 ± 0.006% for F3, 89.15 ± 0.003% for F9 and 82.00 ± 0.002% for F7. The release rate declined between 10 and 24 h, which is consistent with a falling concentration gradient as the drug in the microsponges was depleted. F3 showed the fastest release and the highest burst, followed by F9, which released the drug faster than F7 after 6 h. F7 showed the slowest and most prolonged release throughout the study, with the lowest initial burst (7.85%) and the lowest cumulative release at 24 h (82.00%). As the aim of the formulation was sustained release, F7 was considered the best formulation, since it retained the drug in the microsponges for longer and released it gradually over the 24 h period. This is desirable for maintaining the drug at the wound site for a prolonged time and reducing the dosing frequency.

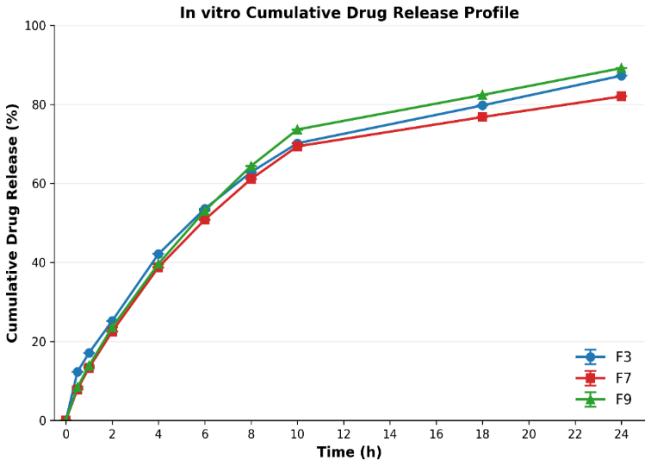

Figure 11: Drug release profile of F3, F7 and F9 MSPG

Drug release kinetics

The coefficient of determination (R2) was taken as the criteria for choosing the most appropriate model. The R2 values of various model fittings of in vitro drug release data of optimized formulation are mentioned in Table 6. The in vitro drug release studies of the optimized PTX-MSPs formulation was best explained by Korsmeyer-Peppas kinetics, as the plot showed R2 value of 0.9666. The value of the release exponent obtained from the Korsmeyer-Peppas model was found to be 0.6332. Since n lies between 0.43 and 0.85, it indicates that the drug release follows an anomalous (Non-Fickian) transport mechanism, where drug dissolution is controlled simultaneously by diffusion through the polymer matrix and polymer swelling chain relaxation.

Table 6: Release kinetics modelling parameters of optimized formulation gel

Model Fitting	Zero order	First order	Higuchi	Korsmeyer-Peppas
R^2	0.8032	0.9314	0.9545	0.9666
k	4.4472	0.0317	18.818	0.6332

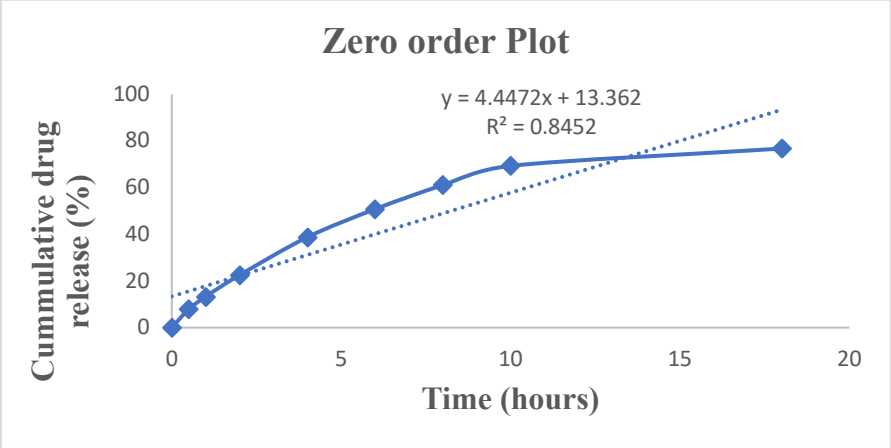

Figure 12: Zero order Plot

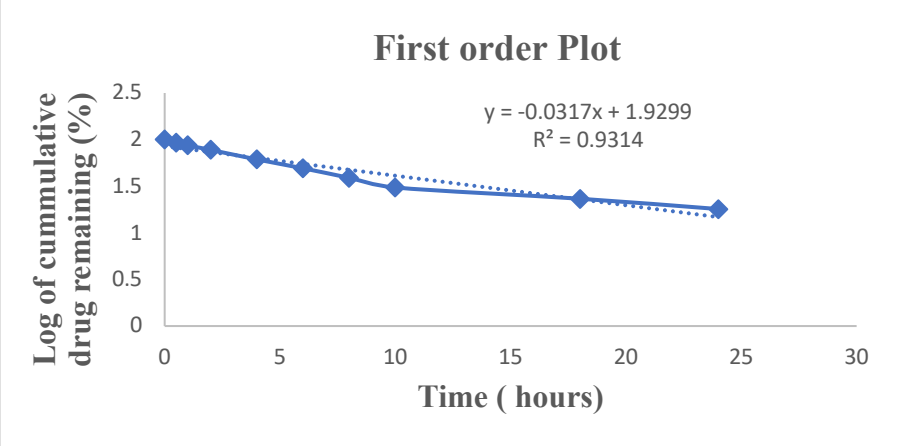

Figure 13: First order plot

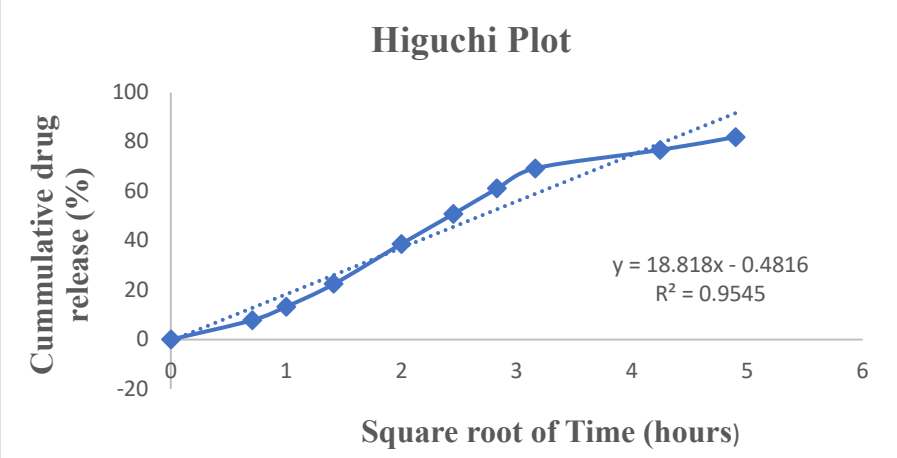

Figure 14: Higuchi Plot

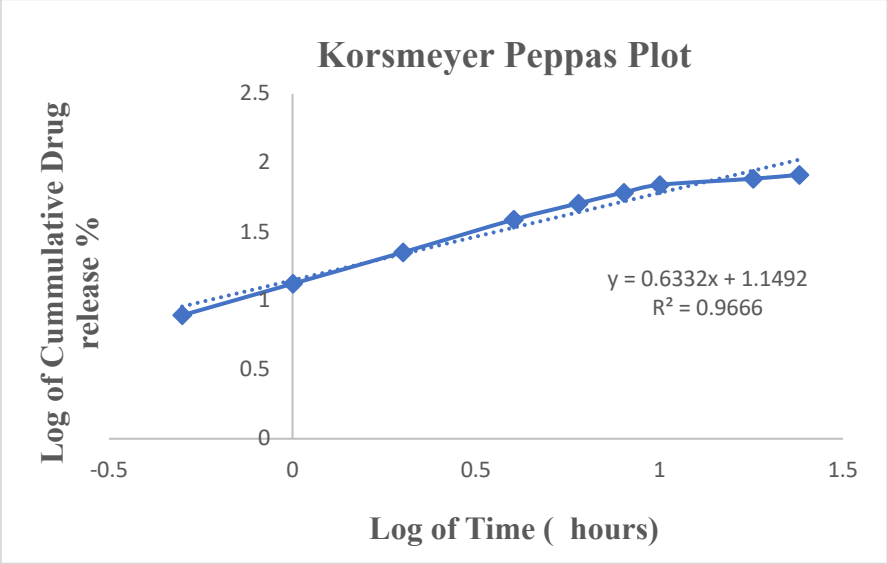

Figure15: Korsmeyer Peppas plot

Stability Studies

The results of the stability study, as shown in Table 7, revealed that the PTX-MSPG gel was found to be stable after a period of three months. Significant changes have not been seen when these were demonstrated for physical appearance, pH, and drug content at different temperature conditions (4 ± 2 ºC, 25 ± 2 ºC and 40 ± 2 ºC).

Table 7: Stability studies data of optimized formulation

Parameters	**PTX- MSs gel**			
	Initial	**After 3 months at 4ºC temperature**	**After 3 months at 25ºC temperature**	**After 3 months at 40ºC temperature**
Physical appearance	Colourless and translucent	No change	No change	No change
pH	6.1	6.1	6.0	6.0
Drug content (%)	92.82% ± 0.97	92.54% ± 0.09	92.17% ± 0.17	90.66% ± 0.63

Skin irritation study

The skin irritation potential of the formulations was evaluated in rats using the Draize scoring method (Table 8), and the primary irritation index (PII) was calculated as the sum of the mean erythema and mean edema scores (n = 6 per group). The untreated control group showed no erythema or edema, whereas formalin (positive control) produced severe and consistent reactions (erythema 3.50 ± 0.55, edema 3.33 ± 0.52; PII = 6.83), classifying it as a severe irritant. In contrast, the blank microsponge gel produced very slight erythema in only one of six animals (PII = 0.17), and the PTX-loaded microsponge gel produced very slight erythema in two of six animals (PII = 0.33), with no edema observed in either group; both gels had PII values below 0.5 and were classified as non-irritant. Statistical analysis of the total irritation scores by the Kruskal-Wallis test revealed a significant difference among the groups ($H = 18.09$, $p = 0.0004$), and Dunn's multiple comparisons test showed that formalin differed significantly from the control (adjusted $p = 0.0008$), blank gel (adjusted $p = 0.0040$) and PTX gel (adjusted $p = 0.0174$) groups, whereas no significant differences were found among the control, blank gel and PTX gel groups (adjusted $p > 0.9999$). The significant separation of the formalin group confirms the sensitivity of the model in detecting irritation, while the comparable scores of the blank and drug-loaded gels indicate that the polymer, gelling agent and other excipients did not contribute to irritation and that incorporation of pentoxifylline into the microsponges did not alter the safety profile of the base. The negligible reactions observed with the PTX-MSs gel may also be attributed to the gradual release of the drug from the porous microsponge structure, which avoids a high concentration of free drug on the skin surface. These findings demonstrate that the PTX-loaded microsponge gel is safe and well tolerated for topical application and supports its further evaluation in wound healing studies.

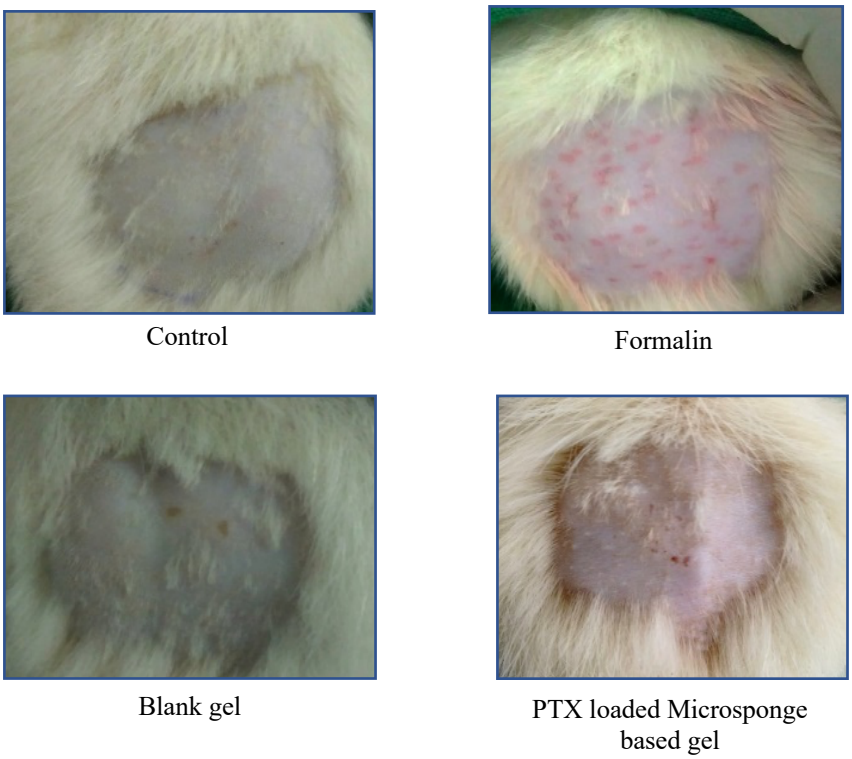

Figure 16: Photographs of rat skin for skin irritation study

Table 8: Skin irritation score of the control, formalin, blank gel and PTX-MSs gel

Rat No.	Control		Formalin		Blank Microsponge based gel		PTX loaded Microsponge based gel	
	Erythema	Edema	Erythema	Edema	Erythema	Edema	Erythema	Edema
1	0	0	3	3	0	0	0	0
2	0	0	4	3	0	0	1	0
3	0	0	3	4	1	0	0	0
4	0	0	4	3	0	0	0	0
5	0	0	4	3	0	0	1	0
6	0	0	3	4	0	0	0	0

***In vivo* studies wound healing studies**

The *in vivo* wound healing potential of the formulated topical preparations was evaluated by measuring the reduction in wound area (Fig.17) and calculating the percentage of wound contraction across four distinct experimental groups over a period of 21 days. The quantitative observations recorded on Days 0, 3, 5, 10, 15, and 21 are summarized in Table 9.

Percentage wound contraction assessment

The wound healing efficacy of the formulations was assessed by measuring wound area and percent wound contraction up to day 21 (Table 9). Initial wound areas were comparable among all groups (1.978-2.030 cm^2), confirming uniform wound creation. Wound contraction progressed with time in every group, but the rate of closure differed markedly between treatments. Group IV (PTX-loaded microsponge gel) showed the fastest healing from the earliest time point, with 24.88% contraction on day 3 compared with 5.05%, 12.63% and 6.89% in Groups I, II and III, respectively. This advantage was maintained on day 5 (46.26% vs 11.99%, 28.41% and 14.28%), day 10 (77.61% vs 27.84%, 53.58% and 30.54%) and day 15 (87.06% vs 44.69%, 79.37% and 46.79%). By day 21, wounds in Group IV were almost completely closed (98.01%), with a residual area of only 0.040 ± 0.005 cm^2, whereas contraction was 91.15% in Group II and 67.88% and 69.95% in Groups I and III, respectively. The nearly identical healing profiles of Groups I and III indicate that the blank gel base had no appreciable effect on wound closure. Two-way ANOVA showed that time, treatment

and their interaction all had significant effects on wound contraction ($p < 0.0001$), indicating that the healing trajectory depended on the treatment applied.

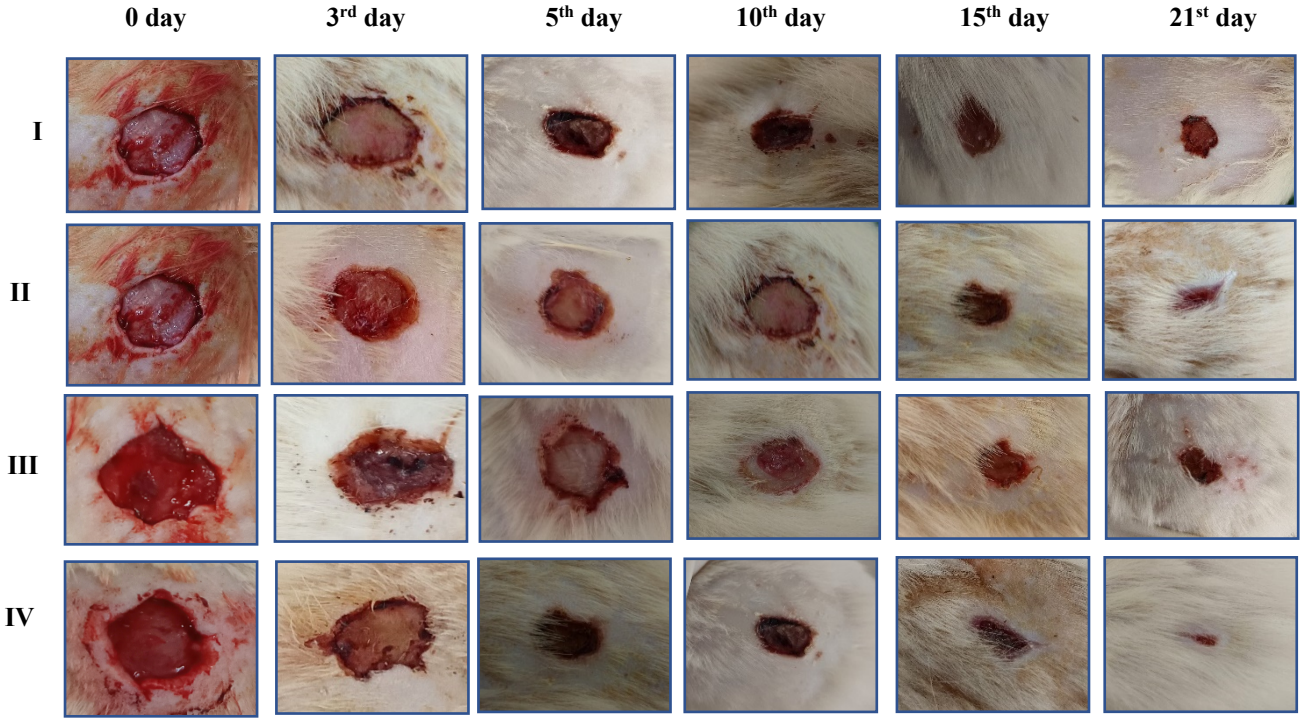

Figure 17: Photographic representation of wound healing and wound closure in rats

Table 9: Tabular representation of percentage wound closure

Days	Group I		Group II		Group III		Group IV	
	Area (cm^2)	% contraction	Area (cm^2)	% contraction	Area (cm^2)	% contraction	Area (cm^2)	% contraction
0	2.018 ± 0.049	0	1.978 ± 0.053	0	2.03 ±0.054	0	2.010 ± 0.039	0
3	1.916 ± 0.038	5.05	1.728 ± 0.048	12.63	1.890 ± 0.054	6.89	1.510 ± 0.037	24.88
5	1.776 ± 0.040	11.99	1.416 ± 0.043	28.41	1.740 ± 0.046	14.28	1.080 ± 0.033	46.26
10	1.456 ± 0.043	27.84	0.918 ± 0.041	53.58	1.410 ± 0.040	30.54	0.450 ± 0.024	77.61
15	1.116 ± 0.040	44.69	0.408 ± 0.026	79.37	1.080 ± 0.039	46.79	0.260 ± 0.023	87.06
21	0.648 ± 0.057	67.88	0.175 ± 0.135	91.15	0.610 ± 0.031	69.95	0.040 ± 0.005	98.01

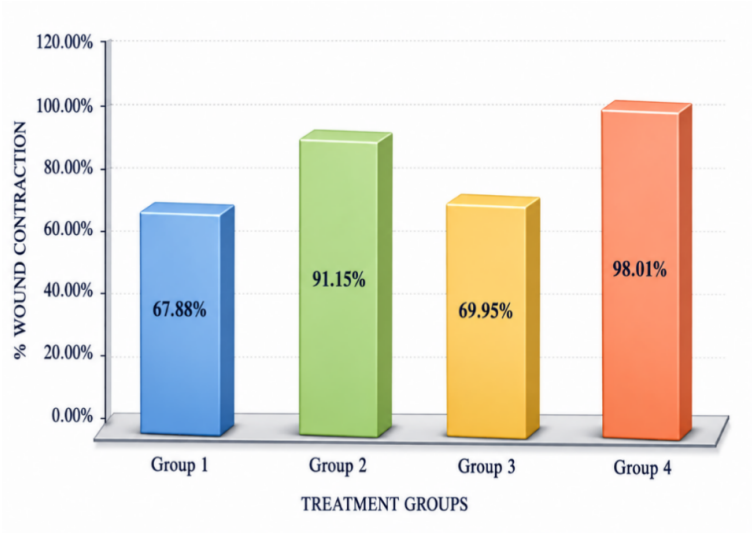

Figure 18: Graphical representation of % wound closure in wistar rats in different treatment groups

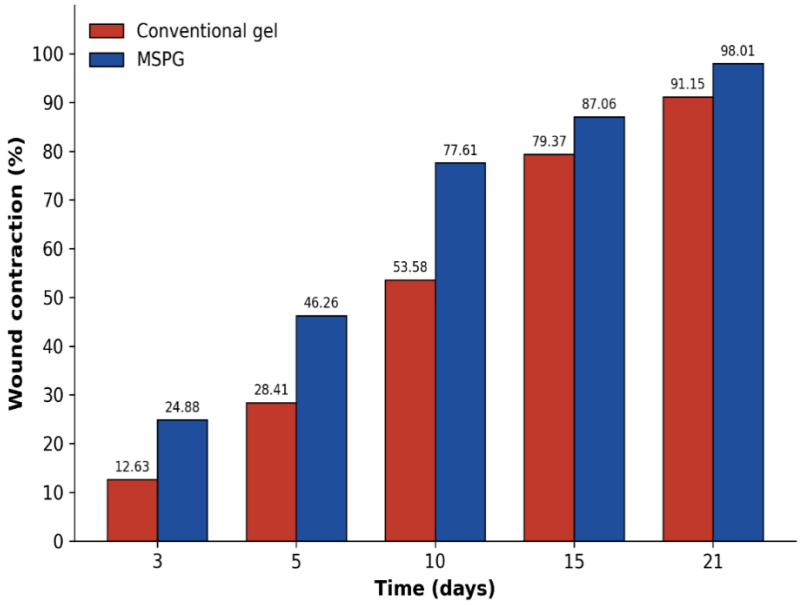

Figure 19: Percent wound contraction in rats treated with conventional gel and MSPG over 21 days

Histopathological Evaluation

The normal architecture of skin tissue without any inflammatory infiltration and cellular necrosis is shown in Fig. 19 (a). Whereas the presence of edema, monocyte cells, cellular necrosis, aggregation of macrophages, and poor collagenation with large numbers of fibroblasts were characteristic features of the delayed in wound healing processes which were observed in the skin tissue from vehicle control rats. Histopathological examination of the untreated wound tissue on Day 21 shown in Fig. 19 (b) revealed features of chronic dermatitis, characterized by irregular epidermal hyperplasia, dermal fibroplasia, persistent neovascularization, less organized collagen and a diffuse mononuclear inflammatory infiltrate. No evidence of complete epidermal maturation, dense collagen remodelling, or resolution of inflammation was observed. This indicates that, in the absence of treatment, the wound healing process remained incomplete and histologically active even at Day 21, reflecting a delayed and prolonged inflammatory-reparative response. Treatment with PTX loaded microsponges gel resulted in minimal inflammatory infiltrate, relatively thin and well-matured keratinising epidermis, consistent with complete re-epithelialisation. Dermis showed relatively mature, thick and organised collagen bundles with low fibroblastic cellularity. Fig. 19 (c) indicates the advance healing with predominant remodelling and maturation.

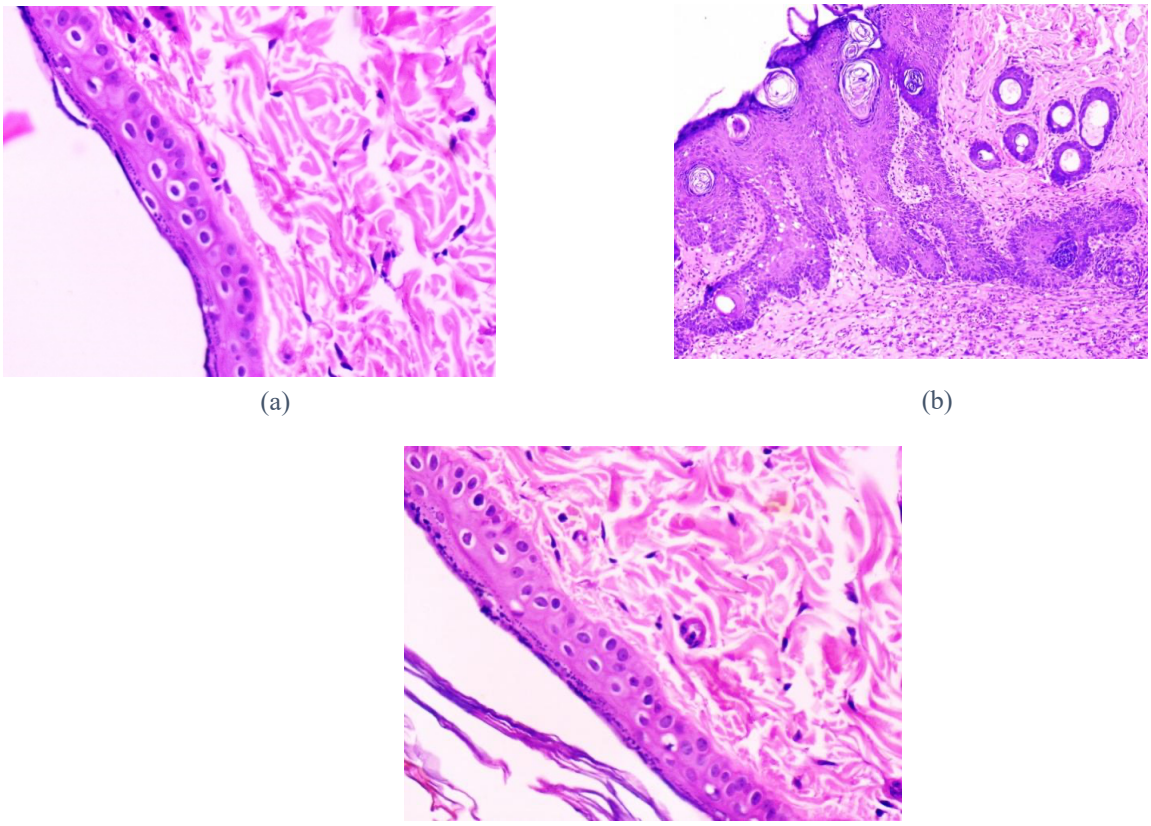

(a) (b)

(c)

Figure 19: Histopathological evaluation of rat skin on day 21 (a) Normal (b) Untreated (c) Treated

CONCLUSION

Pentoxifylline-loaded ethyl cellulose microsponges were successfully developed by the quasi-emulsion solvent diffusion method and optimised using a central composite design. The optimised microsponges showed high entrapment efficiency (88.6 ± 0.8%) and a spherical, porous structure, with the drug present in a non-crystalline state. When incorporated into a Carbopol gel, the system showed acceptable physicochemical properties, good stability, sustained drug release and no skin irritation. In the excision wound model, the microsponge gel gave greater wound contraction (98.01% on day 21) than the conventional PTX gel (91.15%), and histopathology confirmed improved tissue repair. Thus, the PTX-loaded microsponge gel is a safe and effective sustained-release topical system for wound healing. Studies in chronic wound models and clinical trials are warranted to confirm these findings.

ABBREVIATIONS

PTX	Pentoxifylline
EC	Ethyl cellulose
DCM	Dichloromethane
PVA	Polyvinyl alcohol
MSPs	Microsponges
I.P.	Intraperitoneal
PTX-MSPs	Pentoxifylline microsponges
PTX-MSPG	Pentoxifylline microsponge based gel
ANOVA	Analysis of variance
FT-IR	Fourier Transform Infrared
DSC	Differential scanning calorimetry
SEM	Scanning electron microscopy
%PY	Per cent production yield
%EE	Per cent entrapment efficiency
PII	Primary Irritation Index
cPs	Centipoise
mL	Millilitre
min	Minutes
hrs	Hours
g	Gram
µm	Micrometre
rpm	Rotation per minute
°C/min	Degree Celsius per minute
cm	Centimetre
cm^{-1}	Per centimetre

ACKNOWLEDGEMENTS

The authors are thankful to Faculty of Pharmacy, Uttar Pradesh University of Medical Sciences, Saifai, Etawah for providing all necessary facilities. Bakul Fine Pharma, Maharashtra is gratefully acknowledged for providing PTX as a gift sample.

AUTHOR CONTRIBUTIONS

KR: conceptualization, methodology, investigation, formal analysis, data curation, visualization, surgical and medical practices, writing original draft; SK: supervision, project administration, validation, and editing; AS: surgical and medical practices; AJ: Literature review, analysis & interpretation.

FUNDING

Not applicable

AVAILABILITY OF DATA AND MATERIALS

All data and material are available upon request.

ETHICS COMMITTEE APPROVAL

The manuscript is solely submitted to this journal and has not been sent elsewhere simultaneously. The content is original, never published before, and complies with ethical standards. Results are presented transparently, without manipulation. Data acquisition adheres to discipline-specific guidelines. The study's experimental procedure received approval from the Institutional Animal Ethics Committee, Department of Animal House, UPUMS, Saifai, Etawah (Approval number IAEC/09/AH/2025-26), following Indian Committee for the Purpose of Control and Supervision of Experiments with Animals (CPCSEA) specifications.

CONSENT FOR PUBLICATION

Yes

CONFLICT OF INTERESTS

The authors declare that they have no conflict of interests.

REFERENCES

1. Criollo-Mendoza MS, Contreras-Angulo LA, Leyva López N, Gutiérrez-Grijalva EP, Jiménez-Ortega LA, Heredia JB. Wound healing properties of natural products: mechanisms of action. Molecules. 2023;28(2):598.

2. Monaco JL, Lawrence WT. Acute wound healing: an overview. Clin Plast Surg. 2003;30(1):1-12.

3. Zeng R, Lin C, Lin Z, Chen H, Lu W, Lin C, et al. Approaches to cutaneous wound healing: basics and future directions. Cell Tissue Res. 2018;374(2):217-32.

4. Sen CK. Human wounds and its burden: an updated compendium of estimates. Adv Wound Care. 2019;8(2):39-48.

5. Gupta N, Gupta SK, Shukla VK, Singh SP. An Indian community-based epidemiological study of wounds. J Wound Care. 2004;13(8):323-5.

6. Sharma A, Srivastava V, Shankar R, Yadav AK, Ansari MA, Gupta SK. Epidemiological profile of chronic wounds in an Indian population: a community-based cross-sectional observational study. Cureus. 2024;16(9):e68684.

7. Embil K, Nacht S. The Microsponge Delivery System (MDS): a topical delivery system with reduced irritancy incorporating multiple triggering mechanisms for the release of actives. J Microencapsul. 1996;13(5):575-88.

8. Osmani RAM, Aloorkar NH, Ingale DJ, Kulkarni PK, Hani U, Bhosale RR, et al. Microsponges based novel drug delivery system for augmented arthritis therapy. Saudi Pharm J. 2015;23(5):562-72.

9. Ward A, Clissold SP. Pentoxifylline. A review of its pharmacodynamic and pharmacokinetic properties, and its therapeutic efficacy. Drugs. 1987;34(1):50-97.

10. Doherty GM, Jensen JC, Alexander HR, Buresh CM, Norton JA. Pentoxifylline suppression of tumor necrosis factor gene transcription. Surgery. 1991;110(2):192-8.

11. Jull AB, Arroll B, Parag V, Waters J. Pentoxifylline for treating venous leg ulcers. Cochrane Database Syst Rev. 2012;(12):CD001733.

12. Beermann B, Ings R, Månsby J, Chamberlain J, McDonald A. Kinetics of intravenous and oral pentoxifylline in healthy subjects. Clin Pharmacol Ther. 1985;37(1):25-8.

13. Nacht S, Katz M. The microsponge: a novel topical programmable delivery system. In: Osborne DW, Amann AH, editors. Topical drug delivery formulations. New York: Marcel Dekker; 1990. p. 299-325.

14. Kaity S, Maiti S, Ghosh AK, Pal D, Ghosh A, Banerjee S. Microsponges: a novel strategy for drug delivery system. J Adv Pharm Technol Res. 2010;1(3):283-90.

15. Ramesh GS, Hussain N, Roy S, Kaity S. Composite polymeric microsponge-based long-acting gel formulation for topical delivery of mupirocin. J Appl Polym Sci. 2024;141(8):e54975.

16. Khattab A, Nattouf A. Optimization of entrapment efficiency and release of clindamycin in microsponge based gel. Sci Rep. 2021;11(1):23345.

17. Mehmood Y, Shahid H, ul Huq UI, Rafeeq H, Khalid HM, Uddin MN, et al. Microsponge-based gel loaded with immunosuppressant as a simple and valuable

strategy for psoriasis therapy: determination of pro-inflammatory response through cytokine IL-2 mRNA expression. Gels. 2023;9(11):871.

18. Dhamak RS, Salve PS, Tiwari DR, Raut PA, Waghmare DS. Enhanced therapeutic approach for diabetic foot ulcers: comparative study and characterisation of mupirocin-loaded nanosponge gel with marketed formulation for accelerating wound healing and in vivo evaluation. Futur J Pharm Sci. 2024;10(1):33.

19. Halder S, Behera US, Poddar S, Khanam J, Karmakar S. Preparation of microsponge drug delivery system (MSDDS) followed by a scale-up approach. AAPS PharmSciTech. 2024;25(6):162.

20. Ma L, Guo S, Piao J, Piao M. Preparation and evaluation of a microsponge dermal stratum corneum retention drug delivery system for griseofulvin. AAPS PharmSciTech. 2022;23(6):199.

21. Patil A, Masareddy RS, Patil AS, Dwivedi PS. Microsponge gel approach to increase the stability and efficacy of avobenzone as a sun-protective agent. J Pharm Innov. 2022;17(4):1347-59.

22. Rekhi GS, Jambhekar SS. Ethylcellulose - a polymer review. Drug Dev Ind Pharm. 1995;21(1):61-77.

23. Shiehzadeh F, Mohebi D, Chavoshian O, Daneshmand S. Formulation, characterization, and optimization of a topical gel containing tranexamic acid to prevent superficial bleeding: in vivo and in vitro evaluations. Turk J Pharm Sci. 2023;20(4):261.

24. Kaplan AB, Cetin M, Orgul D, Taghizadehghalehjoughi A, Hacımuftuoglu A, Hekimoglu S. Formulation and in vitro evaluation of topical nanoemulsion and nanoemulsion-based gels containing daidzein. J Drug Deliv Sci Technol. 2019;52:189-203.

25. Wang E, Qi Z, Cao Y, Li R, Wu J, Tang R, et al. Gels as promising delivery systems: physicochemical property characterization and recent applications. Pharmaceutics. 2025;17(2):249.

26. Aiyalu R, Govindarjan A, Ramasamy A. Formulation and evaluation of topical herbal gel for the treatment of arthritis in animal model. Braz J Pharm Sci. 2016;52(3):493-507.

27. Sivadasan D, Venkatesan K, Mohamed JM, Alqahtani S, Asiri YI, Faisal MM, Ibrahim AE, Alrashdi YB, Menaa F, Deeb SE. Application of 32 factorial design for loratadine-loaded nanosponge in topical gel formulation: comprehensive in-vitro and ex vivo evaluations. Scientific Reports. 2024 Mar 16;14(1):6361.

28. Imam SS, Gilani SJ, Zafar A, Jumah MN, Alshehri S. Formulation of miconazole-loaded chitosan-carbopol vesicular gel: optimization to in vitro characterization, irritation, and antifungal assessment. Pharmaceutics. 2023;15(2):581.

29. Bayan MF, Chandrasekaran B, Alyami MH. Development and characterization of econazole topical gel. Gels. 2023;9(12):929.

30. Food and Drug Administration (US). Guidance for industry: Q1A(R2) stability testing of new drug substances and products. Rockville (MD): U.S. Department of Health and Human Services, Food and Drug Administration; 2003.

31. Hajare A, Dol H, Patil K. Design and development of terbinafine hydrochloride ethosomal gel for enhancement of transdermal delivery: in vitro, in vivo, molecular docking, and stability study. J Drug Deliv Sci Technol. 2021;61:102280.

32. Piana M, Silva MA, Trevisan G, de Brum TF, Silva CR, Boligon AA, et al. Antiinflammatory effects of Viola tricolor gel in a model of sunburn in rats and the gel stability study. J Ethnopharmacol. 2013;150(2):458-65.

33. Saeedi M, Morteza-Semnani K, Akbari J, Rahimnia SM, Ahmadi F, Mojaveri MR, et al. Green formulation of menadione-loaded niosome as a skin-lightening preparation: in vitro/in vivo safety evaluation on Wistar rat. Adv Pharm Bull. 2024;14(4):858.

34. Hamad AM, Ahmed HG. Association of some carbohydrates with estrogen expression in breast lesions among Sudanese females. J Histotechnol. 2018;41(1):2-9.

35. Asghar Z, Jamshaid T, Jamshaid U, Madni A, Akhtar N, Lashkar MO, et al. In vivo evaluation of miconazole-nitrate-loaded transethosomal gel using a rat model infected with Candida albicans. Pharmaceuticals. 2024;17(5):546.

36. Kandhare AD, Alam J, Patil MV, Sinha A, Bodhankar SL. Wound healing potential of naringin ointment formulation via regulating the expression of inflammatory, apoptotic and growth mediators in experimental rats. Pharm Biol. 2016;54(3):419-32.